

Cornering Force Maximization with Variable Slip Ratio Control Based on Brush Tire Model

Hiroyuki Fuse¹⁾

Hiroshi Fujimoto¹⁾

1) The University of Tokyo, 5-1-5 Kashiwanoha, Kashiwa, Chiba, 277-8561 Japan

E-mail: fuse.hiroyuki17@ae.k.u-tokyo.ac.jp

ABSTRACT: With the motivation of the enhancement of the controllability of electric vehicles (EVs), this study proposes an effective slip ratio control method of EVs that maximizes cornering force of each wheel. A variable slip ratio limiter (VSRL) is constructed based on brush tire model in order to increase the lateral force of tire. However, a conventional VSRL did not necessarily maximize cornering force since it did not consider the effect of steering angle and cornering drag force. The new VSRL is proposed here with a basic experimental verification using a real EV. The results confirm the increase of both yaw rate and lateral acceleration while turning at the same speed.

KEY WORDS: electric vehicle, slip ratio control, brush model

1. Introduction

Electrification of vehicles has been an utmost priority in the vehicle industries due to the arising environmental problems. Various studies have been conducted in order to electric vehicles (BEVs) such as range extension found in ⁽¹⁾ and ⁽²⁾. On the other hand, BEVs have other advantages in controllability, since electric motor has fast torque response within several milliseconds and the generated torque and driving force acting on the wheel can be easily obtained, and it can be mounted for each wheel with ease, allowing all wheels individually driven ⁽³⁾. These advantages are the most important aspect of the maneuverability of BEVs, and traction control and driving force distribution of each wheel of BEVs are widely investigated ⁽⁴⁾ ⁽⁵⁾.

The group of the author has also been working on these fields. For maximizing the effectiveness of the traction control while maintaining simple structure of the controller, we developed a driving force controller (DFC) ⁽⁶⁾ in 2011. The DFC has wheel speed controller in its inner loop and directly controls slip ratio.

In order to fully maximize the tire force at any situation, Fuse proposed a variable slip ratio limiter (VSRL) considering the lateral slip angle of the wheels for the DFC based on λ -Method tire model ⁽⁷⁾. Then, the VSRL based on brush tire model was proposed afterwards so that wider types of tires can be handled ⁽⁸⁾. However, when the sideslip angle is too large, the slip ratio (i.e. longitudinal slip) is limited to zero by the VSRL and the maximization of the cornering force (perpendicular to the body speed vector) cannot be achieved.

The newly proposed VSRL increases cornering force in case the sideslip angle of the wheel is very large. The effectiveness of the newly proposed VSRL is demonstrated by an experiment using a real EV, with the increase of yaw rate and lateral acceleration.

2. Vehicle model

2.1. Simplified vehicle model

In this paper, we consider a vehicle model whose wheels are individually driven. Fig. 1 shows an illustration of the vehicle model. Detailed explanation of the vehicle model will be given in the final manuscript.

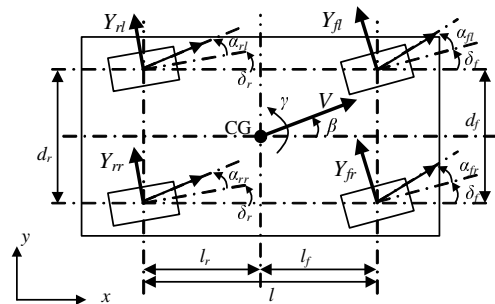


Fig. 1 Vehicle model.

2.2. Tire model

2.2.1. Friction circle

Fig. 2(a) shows a simplified tire model to consider. In the figure, J_ω , ω , T , r , F , N , θ , and μ_{\max} are inertia of wheel, angular velocity, torque input by traction motors, radius of tire, resultant force of the tire, normal reaction force acting on tire, tire force direction, and the maximum friction coefficient, respectively (subscript ij is omitted in the figure).

2.2.2. Generation of Tire Force

In general, longitudinal and lateral force are generated by slip ratio and sideslip angle respectively. In this paper, slip ratio λ_{ij} is defined by

$$\lambda_{ij} = (V_{\omega_{ij}} - V_{x_{ij}}) / \max(V_{\omega_{ij}}, V_{x_{ij}}), \quad (1)$$

where $V_{\omega_{ij}} = r\omega_{ij}$ and $V_{x_{ij}} = V_{ij} \cos \alpha_{ij}$. The relation between slip ratio λ and friction coefficient of road μ is nonlinear as shown in Fig. 2(b). The friction coefficient takes its maximum value μ_{\max} at a certain slip ratio called optimal slip ratio λ_{p0} when $\alpha = 0$.

2.2.3. Brush Model

Brush model assumes countless number of brush-shaped elastic body continuously on the surface of tire. Tire force and its moment are calculated based on the elastic deformation of the brush. a , b , C_x , C_y denote the length and width of contact area, longitudinal and lateral stiffness of the brush, respectively. By

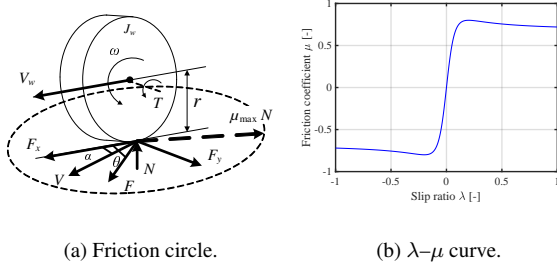


Fig. 2 Tire force model.

assuming that the longitudinal and lateral pressure distributions of contact area are quadratic and constant respectively, resultant force F , longitudinal force F_x , and lateral force F_y of tire are obtained as follows⁽⁹⁾.

$$F(\lambda, \alpha) = \mu_{\max} N s (3 - 3s + s^2), [0 \leq s \leq 1] \quad (2)$$

where s is the normalized slip. When $s = 0$, tire is completely adhesive. When $s = 1$, all the contact patch area becomes slipping. Since the definition of slip ratio differs in case of acceleration and deceleration, s and θ are respectively represented in each case. In case of deceleration, they are given by

$$\theta(\lambda, \alpha) = -\tan^{-1} \left(\frac{\phi \tan \alpha}{\lambda} \right) \quad (3)$$

$$s(\lambda, \alpha) = K \frac{\sqrt{\lambda^2 + \phi^2 \tan^2 \alpha}}{1 + \lambda} \quad (4)$$

$$K := a^2 b C_x / 6 \mu_{\max} N = 1 / \lambda_{p0t}, \quad C_y = \phi C_x \quad (5)$$

where K is a parameter determining s , λ_{p0t} is an optimal slip ratio for driving mode ($\lambda > 0$), and ϕ is a stiffness ratio between longitudinal and lateral direction.

3. Driving Force Controller

Due to the limited space, detailed explanation of the DFC will be given in the final manuscript.

3.1. Block diagram and structure

The block diagram of the DFC is shown in Fig. 3. The feedback loop has a slip ratio controller with a limiter. The definition of slip ratio λ has two cases on both acceleration and deceleration. However, switching between these two is not desired for smooth control, so the slip ratio reference value y is defined as

$$y = (V_\omega - V) / V = \lambda \quad (\lambda < 0). \quad (6)$$

This is the same definition as that of the slip ratio λ for deceleration ($\lambda < 0$). y is used for both acceleration and deceleration solely.

3.2. Previous variable slip ratio limiter

Fuse proposed a variable slip ratio limiter (VSRL) for y according to the change of α_{ij} based on λ -Method tire model⁽⁷⁾ first, and then based on the brush tire model⁽⁸⁾. With the brush tire model, difference between longitudinal and lateral stiffness can be taken into account as ϕ , which achieves more applicability to wider tire types as compared to the λ -Method tire model.

In the previous study⁽⁸⁾, the VSRL based on the brush tire model is given by

$$y_{\max}(\alpha) = (\lambda_{p0t}^2 + X_1) / (1 - \lambda_{p0t}^2) \quad (|\alpha| \leq \alpha_{\max}) \quad (7)$$

$$y_{\min}(\alpha) = (\lambda_{p0t}^2 - X_1) / (1 - \lambda_{p0t}^2) \quad (|\alpha| \leq \alpha_{\max}) \quad (8)$$

$$X_1 := \sqrt{\lambda_{p0t}^2 + (\lambda_{p0t}^2 - 1) \phi^2 \tan^2 \alpha} \quad (9)$$

$$\alpha_{\max} := \tan^{-1}(\lambda_{p0t}) / (\phi \sqrt{1 - \lambda_{p0t}^2}) \quad (10)$$

With the VSRL, the normalized slip s is always kept within 1 ($s \leq 1$) so that tire force is effectively maximized for both longitudinal and lateral directions as long as $|\alpha| \leq \alpha_{\max}$ satisfies.

In the previous study, in case of large sideslip angle $|\alpha| > \alpha_{\max}$, which means that lateral slip is so large that all the contact patch area slips regardless of longitudinal slip (slip ratio λ), $y_{\max} = y_{\min} = 0$ was adopted so that the largest lateral force can be achieved.

4. Proposal of a new variable slip ratio limiter

4.1. Problem with the conventional variable slip ratio limiter

The previous VSRL did not consider the effect of the steering angle δ_f and body sideslip angle β . Therefore, the cornering force, which is perpendicular to the direction of the body speed vector, would not necessarily be maximized and the part of the lateral force of the tire works as a cornering drag force due to the steering angle δ_f and body sideslip angle β , especially in case of large sideslip angle α .

In the previous VSRL, when $|\alpha_{ij}| > \alpha_{\max}$, the DFC limits the slip ratio λ_{ij} to be zero. The tire force vector faces diagonally backward by α_{ij} from the direction perpendicular to the body speed vector V_{ij} (shown as "conv. VSRL" in Fig. 4). The longitudinal component with respect to the V_{ij} works as cornering drag force, which is $F_{ij} \sin \alpha_{ij}$. On the other hand, a newly proposed VSRL changes the slip ratio limiter so that the tire force direction becomes perpendicular to the body speed vector V_{ij} (shown as "prop. VSRL" in Fig. 4), effectively maximizing the cornering force while decreasing the undesired longitudinal drag force by $F_{ij} \sin \alpha_{ij}$.

4.2. Cornering force maximization method

This section derives a desired slip ratio so that the tire force direction becomes perpendicular to the body speed vector and the cornering force can be effectively maximized. First, we define ξ_{ij} that represents the angle between V_{ij} and V , which is given by

$$\xi_{ij} = \delta_f + \alpha_{ij} - \beta \quad (11)$$

The desired tire force direction θ_{ij-CFM} that faces perpendicular to the body speed vector V is given by

$$\theta_{ij-CFM} = \pi/2 + \alpha_{ij} - \xi_{ij} \quad (12)$$

Here, α_{ij} and $\theta = \theta_{ij-CFM}$ are given so that we can calculate the desired slip ratio λ_{ij-CFM} by substituting these values to (3) as follows.

$$\lambda_{ij-CFM} = \phi \tan \alpha_{ij} \tan(\alpha_{ij} - \xi_{ij}) \quad (13)$$

Since we used the formula of the brush tire model in case of deceleration for the derivation, we can directly use λ_{ij-CFM} as y_{ij-max} and y_{ij-min} .

4.3. Limiter-switching sideslip angle

The next thing to be done is to obtain the limiter-switching sideslip angle α_{sw} where the VSRL will be switched from the conventional one to the newly proposed one. When $\alpha = \alpha_{sw}$, two relations $s = 1$ (condition of the original VSRL where the

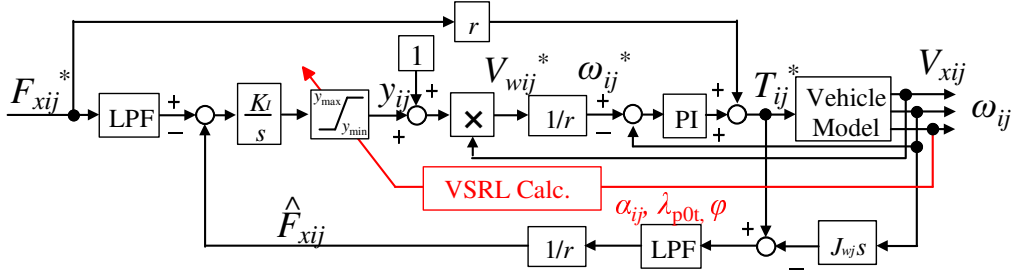


Fig. 3 Driving Force Controller with proposed variable slip ratio limiter.

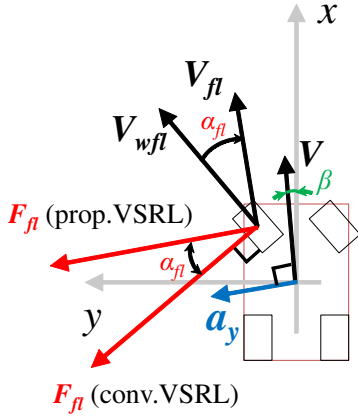


Fig. 4 The proposed VSRL faces the tire force direction perpendicular to the body speed vector by changing the slip ratio limiter, effectively increasing the cornering force.

tire force becomes maximized) and $\lambda = \lambda_{ij-CFM}$ (condition of the cornering force maximization) are satisfied simultaneously. Unfortunately, a certain combination of λ_{sw} and α_{sw} satisfying the two relations is hard to obtain analytically. However, by assuming $\phi = 1$ (having the equal stiffness for both the longitudinal and lateral direction) and $\xi = 0$ ($V_{ij} = V$) for simplicity (reasonable approximations for the most situations), we can obtain the approximated value of α_{sw} . With $\phi = 1$ and $\xi = 0$, the two relations are represented as follows.

$$s = 1 = \frac{\sqrt{\lambda_{CFM}^2 + \phi^2 \tan^2 \alpha_{sw}}}{\lambda_{p0t}(1 + \lambda_{CFM})} \quad (14)$$

$$\lambda_{CFM} = \tan \alpha_{sw}^2 \quad (15)$$

By substituting (15) to (14), the limiter-switching angle α_{sw} is obtained as

$$\alpha_{sw} = \tan^{-1}(\lambda_{p0t}/\sqrt{1 - \lambda_{p0t}^2}) = \alpha_{max} \quad (16)$$

This suggests that the limiter-switching angle α_{sw} and α_{max} are equal, conveniently. Therefore, the newly proposed VSRL limits the slip ratio λ as shown in (7) and (8) when $|\alpha_{ij}| \leq \alpha_{max}$, as the same with the previous VSRL. On the other hand, when $|\alpha_{ij}| > \alpha_{max}$, the proposed VSRL limits the slip ratio reference values as shown in the following.

$$y_{ijmax} = y_{ijmin} = \phi \tan \alpha_{ij}^2 \quad (|\alpha_{ij}| > \alpha_{max}) \quad (17)$$

From now on, the newly proposed VSRL ((7), (8), and (17)) is noted as VSRL-CFM (CFM for Cornering Force Maximization).

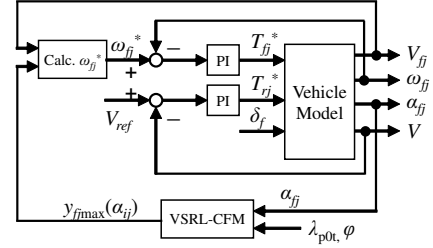


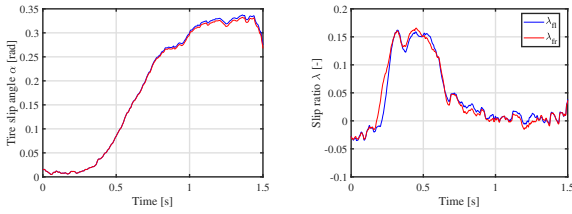
Fig. 5 VSRL-CFM controller and body speed controller for the experimental verification.

5. Experimental Verification

An experimental verification of the VSRL-CFM was conducted using our experimental EV. The EV approached to a slippery road and made a right turn with gradually increasing steering angle (manually done by a driver) while the front wheels were driven by a slip ratio controller with the proposed VSRL-CFM, and the rear wheels were driven by a body speed controller to maintain a constant speed of $V_{ref} = 6$ m/s. At first, front wheels are driven with the slip ratio reference at the optimal slip ratio λ_{p0t} , but as sideslip angle α_{fj} increases with the increasing steering angle, the VSRL-CFM reduces the limiter. After reaching the limiter-switching sideslip angle $\alpha_{sw} = \alpha_{max}$, the VSRL-CFM starts to increase the limiter so that the cornering force can be maximized. The slip ratio reference and the VSRL-CFM were set with $\lambda_{p0t} = 0.16$ and $\phi = 1.14$ which were obtained in advance^{(8) (10)}. For comparison, the same cornering experiment was tested with the conventional VSRL.

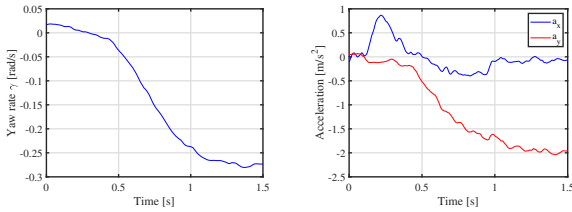
5.1. Experimental results

Experimental results are shown in Fig. 6 and Fig. 7. Sideslip angle α_{fj} increases over 0.3 rad, larger than the limiter switching sideslip angle $\alpha_{sw} \approx 0.18$ (Fig. 6(a) and Fig. 7(a)). Slip ratio λ_{fj} once decreases from 0.16 (λ_{p0t}) but then increases again from around 0.85 s in case of the proposed VSRL-CFM (Fig. 7(b)), while it is maintained around zero in case of the conventional VSRL (Fig. 7(b)). Yaw rate γ in case of the proposed VSRL-CFM reaches to larger (in case of the right turn, they become larger in negative values) value compared to the conventional VSRL and the proposed VSRL-CFM (Fig. 6(c) and Fig. 7(c)). Lateral acceleration a_y (Fig. 6(d) and Fig. 7(d)) seem to settle in the same values around -2 m/s². However, in case of the proposed VSRL-CFM, a_y once reached to -2.3 m/s² so that we can conclude that the proposed VSRL-CFM achieves greater lateral acceleration. If we could have done the same experiment with longer slippery road and measured the steady state longer, we might have seen the clear difference. The increase of yaw rate γ and lateral ac-



(a) Sideslip angle α .

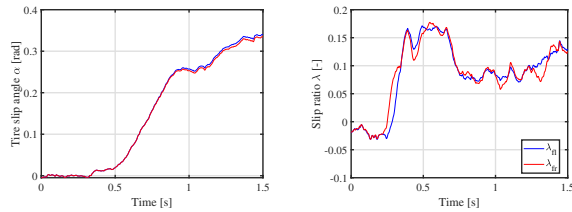
(b) Slip ratio λ .



(c) Yaw rate γ .

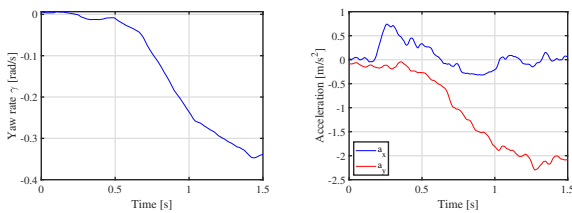
(d) Acceleration.

Fig. 6 Experimental results (Conventional VSRL).



(a) Sideslip angle α .

(b) Slip ratio λ .



(c) Yaw rate γ .

(d) Acceleration.

Fig. 7 Experimental results (Proposed VSRL-CFM).

celeration a_y while on the same speed clearly demonstrates improvements of the maneuverability. Therefore, the newly proposed VSRL works well during the cornering with large sideslip angle α .

6. Conclusion

This study proposed an improved variable slip ratio limiter (VSRL) for traction control of BEVs, in the view of realizing better maneuverability for further development of BEVs. While the conventional VSRL limited the slip ratio reference to be zero when sideslip angle is large in order to achieve greater lateral force for cornering. However, the tire force generated by the conventional VSRL faced backwards when fully activated, causing

some cornering drag and cornering force cannot be maximized. This paper suggested a new method to determine the VSRL based on brush tire model so that the tire force face perpendicular to the body speed vector, effectively maximizing cornering force. The experimental result using a real EV showed increase of cornering force, along with the increase of yaw rate, lateral acceleration, and body sideslip angle.

Acknowledgement

This research was partly supported by Industrial Technology Research Grant Program from New Energy and Industrial Technology Development Organization of Japan (05A48701d), the Ministry of Education, Culture, Sports, Science and Technology grant (22246057 and 26249061).

References

- (1) Y. Ikezawa, et. al., "Range Extension Autonomous Driving for Electric Vehicles Based on Optimal Velocity Trajectory Generation and Front-Rear Driving-Braking Force Distribution," IEEJ J. Industry Applications, vol. 5, no. 3, pp. 228–235, 2016.
- (2) G. Lovison, et. al., "Secondary-side-only Control for High Efficiency and Desired Power with Two Converters in Wireless Power Transfer Systems," IEEJ J. Industry Applications, vol. 6, no. 6, pp. 473–481, 2017.
- (3) Y. Hori, "Future vehicle driven by electricity and control research on four-wheel-motored "UOT electric march II"" , IEEE Trans. Industrial Electronics, 51, 5, pp. 954-962 (2004).
- (4) S. Motoki, O. Yoshiaki, and Nagai, Masao: "Wheel Velocity Control of Micro-Scale Electric Vehicle for Improving Directional Stability", Transactions of the Japan Society of Mechanical Engineers Series C. 70. 1680-1686. 10.1299/kikaic.70.1680, 2004 (in Japanese).
- (5) K. Shi, X. Yuan, G. Huang and Z. Liu, "Compensation-Based Robust Decoupling Control System for the Lateral and Longitudinal Stability of Distributed Drive Electric Vehicle," in IEEE/ASME Transactions on Mechatronics, vol. 24, no. 6, pp. 2768-2778, Dec. 2019.
- (6) M. Yoshimura and H. Fujimoto, "Driving torque control method for electric vehicle with in-wheel motors" , IEEJ Transactions on Industry Applications, Vol. 131, No. 5, pp.1-8 (2010) (in Japanese).
- (7) H. Fuse, H. Fujimoto. "Fundamental Study on Driving Force Control Method for Independent-Four-Wheel-Drive Electric Vehicle Considering Tire Slip Angle" , IEEE conference IECON 2018, 2018.
- (8) H. Fuse, H. Fujimoto: "Driving Force Controller Considering Lateral Slip based on Brush Model for Traction Control of Independent-Four-Wheel-Drive Electric Vehicle", IEEJ Transactions on Industry Applications Vol.140 No.4, pp.1-8, 2020 (originally in Japanese and also translated in English).
- (9) O. Nishihara, et.al., "Estimation of Road Friction Coefficient Based on the Brush Model", Transactions of the Japan Society of Mechanical Engineers Series C 75(753), 1516-1524, 2009. (in Japanese).
- (10) H. Fuse, et.al., "Minimum-time Maneuver and Friction Coefficient Estimation Using Slip Ratio Control for Autonomously-Driven Electric Vehicle" , IEEJ SAM-CON2018, 2018.